Monitoring biophysical parameters of irrigated rice production in the lowlands of the Aral Sea Basin from space

Shavkat Kenjabaev[1], Olga Degtyareva[2], Murodjon Sultanov[3], Michael Thiel[4], Christopher Conrad[4,5]

[1]Scientific Information Center Interstate Coordination Water Commission (SIC ICWC), 100000 Tashkent, Uzbekistan; [2]National Center of Space Research and Technology (NCSRT), 050010 Almaty, Kazakhstan; [3]Khorezm Rural Advisory Support Service (KRASS), 220100 Urgench, Uzbekistan; [4] University of Würzburg, Institute of Geography and Geology, Department of Remote Sensing, 97074 Würzburg, Germany; [5] University of Halle, Institute of Geosciences and Geography, 06120 Halle, Germany.

Introduction

Cultivated mainly in the irrigated lowlands of the Aral Sea Basin (ASB), rice (*Oryza sativa L.*) is one of the most important staple food crops in Central Asia. However, a high risk of crop failure exist because of the exposure to water scarcity and land degradation in these downstream locations. Regional monitoring of rice biophysical parameters is needed which remains a challenging task due to different timings of growth stages under varying management practices and local crop-planting schedules. In this study, statistical relations between vegetation indices (VIs) from Landsat 8 data and biophysical *in situ* measurements (plant height, crop density, green biomass, fraction of absorbed photosynthetically active radiation and leaf area index, LAI) of broadcast sown and transplanted rice were investigated. Special attention laid on the accurate derivation of the LAI owing to its rapid response to different stress factors and changes in climatic conditions.

Study area

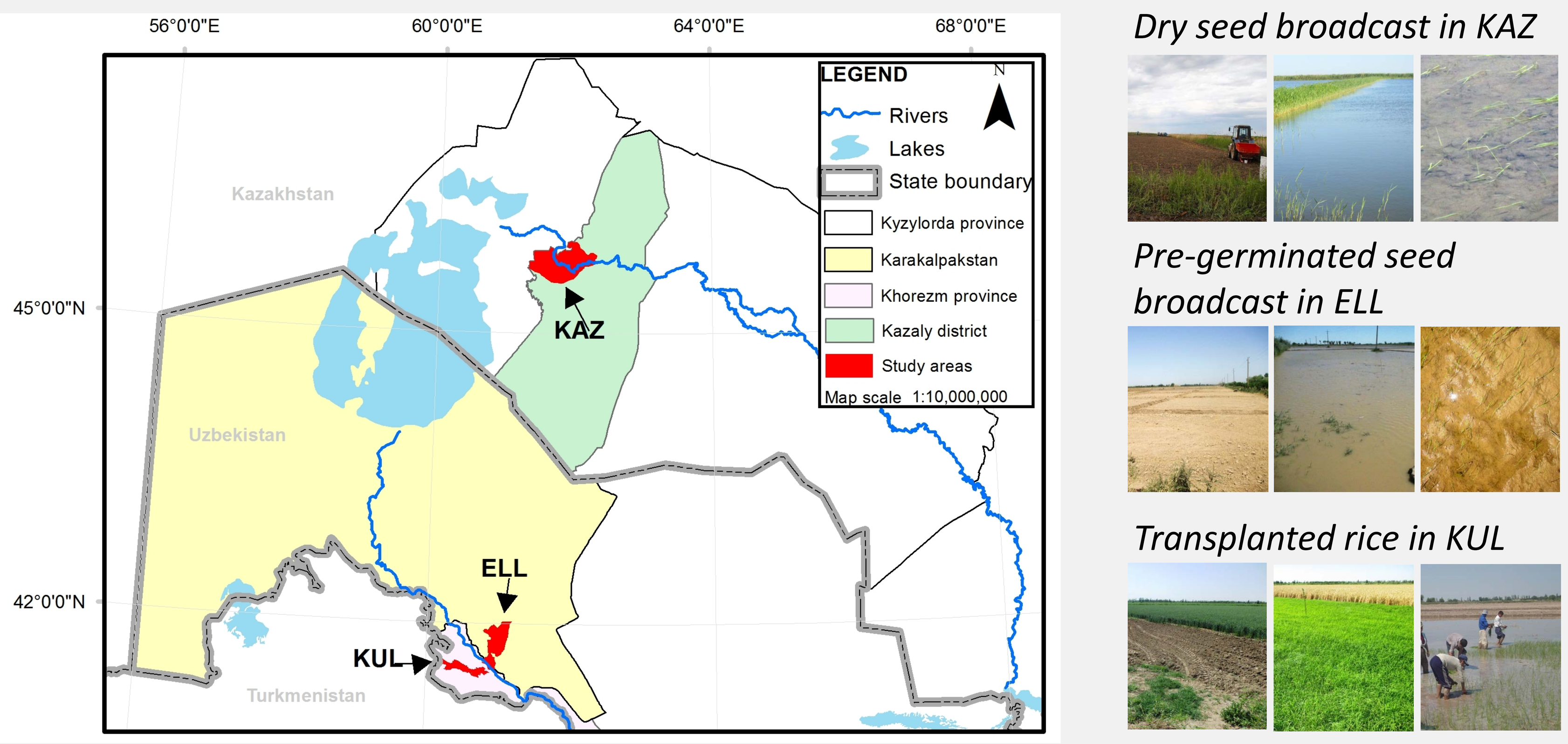

Figure 1: Map of the study sites in the lowlands of the Aral Sea basin (left), photographs of different planting methods of rice (right)

The study sites are located in Kazalinsk district (KAZ), Kyzylorda province, Kazakhstan; Ellikkala district (ELL), Karakalpakstan and Kulavat canal command area (KUL), Khorezm province Uzbekistan (**Fig.1**). Main characteristics of the sites are given in **Table 1**.

Table 1: Main site characteristics, P = precipitation, T = temperature; major rice varieties are underlined

Sites	P, mm	T, °C	Soil texture classes by FAO, %	Field area, ha	Rice varieties	Rice growth period
KAZ	120	8	SL, S (46.6 %), ML (33.1 %), ZL (18.1 %) and others (2.2 %)	2.45±1.46	**Ak-Marzhan**, Yantar, Novator	May-September
ELL	70	14	SL (47.2 %), HL (21.5 %), LL (18.2 %) and ML (13.2 %)	2.19±1.86	**Nukus**, Avabgard, Alanga	June-October
KUL	100	13	ML (36.7 %), LL (31.1 %) and HL (21.0 %)	4.31±2.07	**Alanga**, Avabgard, Lazer	June-September

Results

In situ observations. The mean values of observed rice biophysical parameters for the three sites (**Tab. 2**) revealed enormous spatial variations, both among the fields and sites owing to different land, water and crop management. The site-wise PLHT is variety specific, hence combined with PLDS is influencing on in-situ values of GBMS, FAPAR and LAI.

Table 2: Mean values of rice biophysical parameters during the growing period of rice in study sites.

Biophysical parameters	KAZ			ELL			KUL		
	27.6.-30.6.	27.7.-30.7.	27.8.-30.8.	17.7.-19.7.	20.8.-23.8.	2.10.-3.10.	12.7.-15.7.	15.8.-18.8.	27.9.-30.9.
PLHT (cm)	36	70	90	24	65	69	35	91	93
PLDS* (pl. m^{-2})	175			126			77		
GBMS (g m^{-2})	882	2,091	3,618	944	4,529	884	500	4,210	964
FAPAR (-)	0.22	0.50	0.61	0.32	0.72	0.52	0.12	0.72	0.79
LAI (m^2 m^{-2})	0.46	1.69	2.29	0.79	2.52	2.44	0.28	2.63	2.75

*measured once after singling of plants.

Vegetation indices. The shape of the VIs (2nd order polynomial curve) varies in height and time during the growing period of rice in the sites (**Fig.3**). There are clear shifts of peak values in VIs (e.g., NDGI, RVI and GCI) due to late sowing dates of rice in ELL and KUL sites (~August 9) compared to those in KAZ (~15 days earlier).

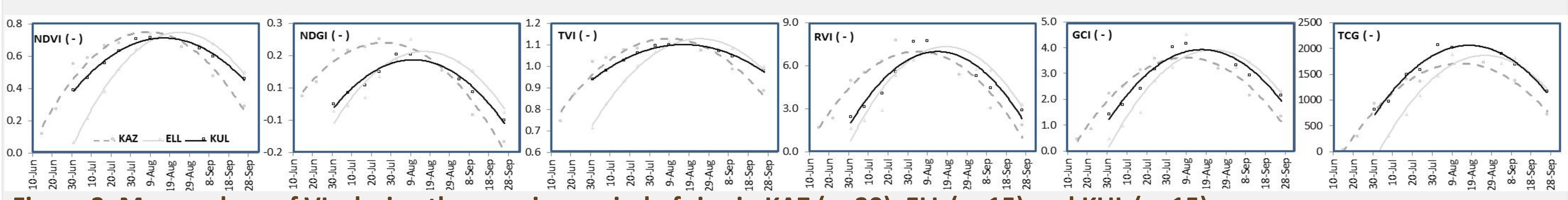

Figure 3: Mean values of VIs during the growing period of rice in KAZ (n=39), ELL (n=15) and KUL (n=15).

Interrelationship between biophysical parameters and VIs. Integrated linear, polynomial (α), power (γ), exponential (δ) and logarithmic (β) relationships (R^2) between all possible pairs of spectro-biophysical parameters for the three sites are given in **Table 3**. The TCG described the LAI better than other VIs: R^2=0.5-0.7 (linear regression) and R^2=0.7-0.8 (polynomial regression).

Table 3: Correlation matrix of the VIs and biophysical parameters for rice in KAZ (A), ELL (B) and KUL (C).

A (n=108)

PLHT	0.42	0.44	0.69	0.67	0.45	0.15	0.44	0.30	0.43	**0.52**
0.60γ	PLDS	0.74	0.36	0.39	0.27	0.03	0.27	0.14	0.28	**0.36**
0.61γ	0.87γ	GBMS	0.40	0.40	0.21	0.05	0.21	0.12	0.20	**0.27**
0.72γ	0.59γ	0.55γ	LAI	0.85	0.57	0.30	0.54	0.51	0.62	**0.71**
0.68δ	0.56	0.53γ	0.95δ	FAPAR	0.66	0.30	0.64	0.49	0.62	**0.67**
0.48δ	0.42δ	0.31δ	0.68δ	0.67α	NDVI	0.56	0.99	0.76	0.87	0.82
0.18α	0.13δ	0.11δ	0.32δ	0.32α	0.56α	NDGI	0.51	0.75	0.58	0.46
0.47δ	0.41δ	0.30δ	0.66δ	0.67α	1.00α	0.72α	TVI	0.70	0.82	0.79
0.50α	0.39γ	0.29γ	0.67γ	0.68α	0.97β	0.76α	0.94β	RVI	0.94	0.80
0.53α	0.40δ	0.30δ	0.65α	0.71α	0.96α	0.60α	0.95α	0.96α	GCI	0.92
0.55α	**0.45δ**	**0.34δ**	**0.71α**	**0.73α**	0.94α	0.46α	0.94α	0.87δ	0.93α	TCG

B (n=39)

PLHT	0.03	0.32	0.76	0.43	0.22	0.09	0.23	0.21	0.26	**0.33**
0.04α	PLDS	0.02	0.01	0.02	**0.14**	**0.14**	**0.14**	0.12	0.13	0.11
0.54γ	0.09γ	GBMS	0.40	0.38	0.35	0.45	0.33	**0.58**	0.50	0.49
0.77δ	0.06α	0.63γ	LAI	0.70	0.41	0.19	0.42	0.35	0.45	**0.54**
0.55δ	0.13α	0.78δ	0.94γ	FAPAR	**0.79**	0.52	**0.79**	0.55	0.67	0.73
0.36γ	**0.16γ**	**0.69δ**	**0.71γ**	**0.84γ**	NDVI	0.75	0.99	0.74	0.86	0.86
0.26α	0.14α	0.55α	0.28α	0.52α	0.75α	NDGI	0.71	0.85	0.76	0.69
0.34γ	**0.16γ**	**0.69δ**	0.63γ	0.79α	1.00α	0.90α	TVI	0.70	0.83	0.84
0.28γ	0.15β	0.66γ	0.44γ	0.73β	0.96β	0.88α	0.93β	RVI	0.93	0.89
0.41γ	0.15γ	0.65γ	0.70γ	0.78α	0.96α	0.76α	0.95α	0.97α	GCI	0.96
0.36δ	0.11α	0.62δ	0.56α	0.80α	0.92α	0.72α	0.92α	0.94α	0.96α	TCG

C (n=45)

PLHT	0.11	0.22	0.82	0.86	0.67	0.39	0.67	0.48	0.63	**0.77**
0.13β	PLDS	0.09	0.03	0.04	0.01	0.01	0.01	0.02	**0.03**	**0.03**
0.47γ	0.13δ	GBMS	0.28	0.23	0.38	**0.56**	0.35	0.48	0.43	0.31
0.85α	0.06α	0.51γ	LAI	0.84	0.64	0.33	0.63	0.46	0.61	**0.74**
0.87α	0.21α	0.47γ	0.97γ	FAPAR	0.79	0.39	0.79	0.44	0.63	**0.84**
0.69α	0.06α	0.55δ	0.79δ	0.79δ	NDVI	0.72	0.99	0.67	0.81	0.92
0.40α	0.02α	**0.62α**	0.39δ	0.41α	0.74α	NDGI	0.67	0.83	0.78	0.64
0.70α	0.06α	0.54δ	**0.80γ**	0.79α	1.00α	0.84α	TVI	0.61	0.77	0.90
0.67β	0.02α	0.57γ	0.70γ	0.72α	0.96β	0.88α	0.93β	RVI	0.95	0.72
0.74α	0.04δ	0.48δ	0.71α	0.84α	0.96α	0.78α	0.94α	0.98α	GCI	0.87
0.78α	**0.09α**	0.43δ	0.76δ	**0.88α**	0.96α	0.66α	0.96α	0.93δ	0.92α	TCG

Multivariate LAI modeling. The evaluation of predicted LAI from NDVI, TVI, GCI and TCG as explaining factors using CART and LM for the three sites are presented in **Table 4**. The CART model explained 92%, 96% and 95% of LAI variability for calibration (75% from total dataset) and 87%, 80% and 95% for validation (25%) in KAZ, ELL and KUL, respectively.

Table 4: Statistical comparisons of observed and modeled LAI using CART and LM (in parenthesis).

Statistical indicators	Calibration			Validation		
	KAZ (n=75)	ELL (n=27)	KUL (n=31)	KAZ (n=32)	ELL (n=12)	KUL (n=14)
R^2	0.92 (0.72)	0.96 (0.80)	0.95 (0.83)	0.87 (0.75)	0.80 (0.73)	0.95 (0.77)
RMSE (m^2 m^{-2})	0.30 (0.55)	0.25 (0.55)	0.33 (0.59)	0.39 (0.55)	0.37 (0.43)	0.26 (0.54)
E (-)	0.92 (0.72)	0.96 (0.80)	0.95 (0.83)	0.87 (0.75)	0.80 (0.73)	0.95 (0.77)
IA (-)	0.96 (0.79)	0.99 (0.92)	0.98 (0.93)	0.94 (0.87)	0.86 (0.86)	0.98 (0.86)

Methods

In situ measurement. Five biophysical parameters were measured at three test plots in each out of 13, 5 and 5 fields in KAZ, ELL and KUL, respectively, and three times during the growing period of rice in 2015:

- plant density (PLDS)
- wet biomass (GBMS)
- plant height (PLHT)
- leaf area index (LAI)
- fraction of absorbed photosynthetically active radiation (FAPAR = 1-(PAR_{bc}/PAR_{ac}))

The device "AccuPAR LP-80" was used to measure LAI and PAR. The sampling scheme is shown in **Fig.2**

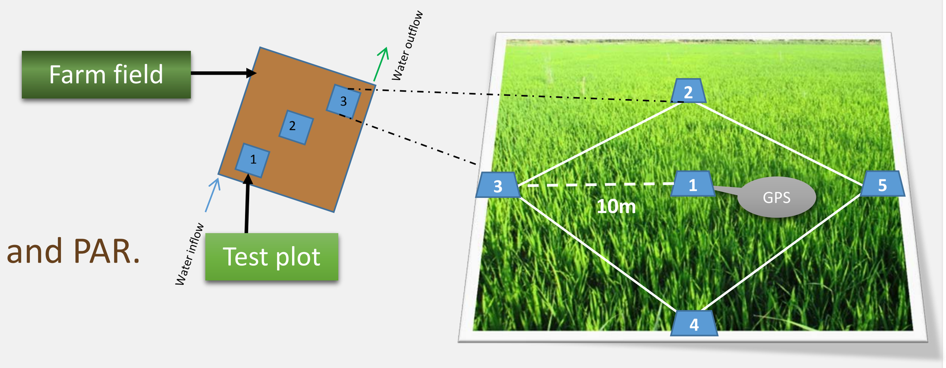

Figure 2: Sampling scheme

Remote sensing data. In total, eighteen scenes of cloud-free Landsat 8 OLI (level-2) archive data in 2015 were downloaded from USGS EarthExplorer (http://earthexplorer.usgs.gov). The broad-band VIs (Pettorelli, 2013), such as Normalized Difference Vegetation Index (NDVI), Normalized Difference Greenness Index (NDGI), Transformed Vegetation Index (TVI), Ratio Vegetation Index (RVI), Green Chlorophyll Index (GCI) and Tasseled Cap Greenness (TCG) were used to identify an optimal predictor of biophysical parameters.

Univariate regression models. Pair-wise spectro-biophysical linear regression analysis (logarithmic, power, exponential and quadratic polynomial) were applied in order to select the best fitting bivariate model.

Multivariate LAI modeling. Two multivariate methods were used to predict LAI:

1) Multivariate linear model (LM) fitted with the *lm* function in the statistical software package R (Fox & Weisberg, 2011): $y = \beta_0 + \sum_{i=1}^{n} \beta_i x_i + \varepsilon$, where y is the target variable, x_i are the explanatory variables (e.g. VIs), β_i are coefficients and ε represents the residual.
2) Classification and Regression Trees (CART, Breiman et al., 1984) using the 'tree' package in R (Ripley, 2007): $\sum_{Y_i|X_{i,j} \le S}(Y_i - \bar{Y})^2 + \sum_{Y_i|X_{i,j} > S}(Y_i - \bar{Y})^2$, where $\bar{Y}$ represents the mean of all elements Y_i for which $X_{i,j}$ is lower than or equal to (greater than) S in the left (right) sum.

Model performance evaluation. Three statistical estimators were used to evaluate the performance of the multivariate models (Green & Stephenson, 1986): (1) the root mean square error (*RMSE*); (2) the coefficient of efficiency (*E*) and (3) the index of agreement (*IA*).

Discussion

Rice biophysical parameters. The FAPAR increases with PLHT (**Fig. 4A**) as well as LAI (**Fig. 4B**) due to the interception of radiation by the crop canopy (Xue et al., 2017). The maximum value of LAI_{max} (4.9 m^2 m^{-2}) is comparable to those published by Ehammer et al. (2010) for the Khorezm condition (also measured through an AccuPAR LP-80 device). Whereas studies by Blenk (2005; LiCOR LAI 2000 and LiCOR LA 3100) & Liu et al. (2017; LiCOR LA 3000) in Khorezm and China, respectively showed higher LAI_{max} values (>6 m^2 m^{-2}) due to fact that both authors used different devices and/or methods.

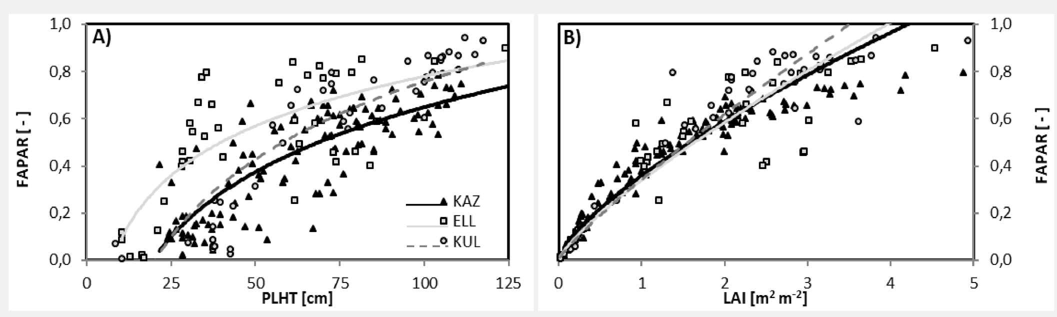

Figure 4: Relationship between FAPAR - (A) with PLHT and – (B) LAI for the growing period of rice in three sites.

Vegetation indices. The temporal pattern of VIs depends upon the phenological stage of rice. Values of VIs increased gradually after rice sowing and reached a plateau by mid to late July in KAZ and early to mid August in ELL and KUL and remained at a high level until late August and mid-September, respectively. As rice plants developed into the ripening in late September to early October, their leaves gradually turned yellowish/golden color, due to a decrease of chlorophyll pigments. Correspondingly, values of VIs declined during this stage.

Univariate LAI modeling. The TCG followed by NDVI, TVI and GCI described the LAI well (and all other biophysical parameters under observation, **Table 3**). NDVI and TVI usually saturate at high LAI therefore follow an exponential curve (**Fig. 5 A&B**), whilst TCG and GCI are not saturating and have a linear relationship (**Fig. 5 C&D**).

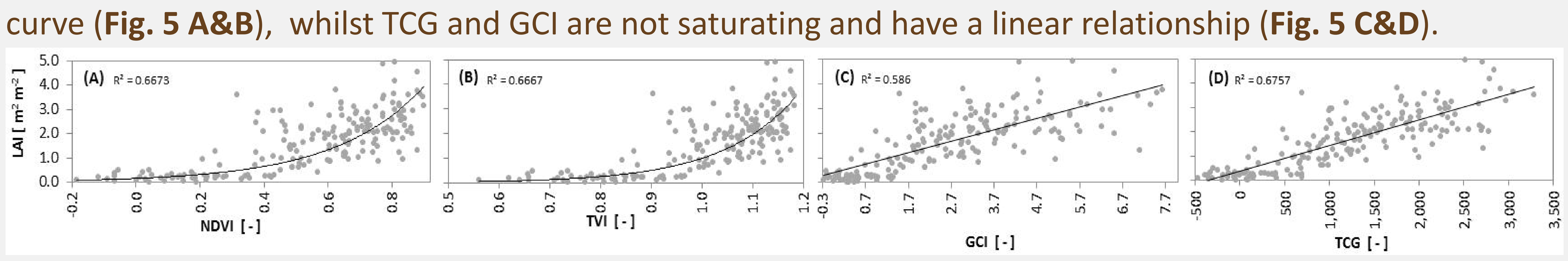

Figure 5: The LAI plotted versus NDVI (A), TVI (B), GCI (C) and TCG (D) for the growing period of rice in three sites.

Multivariate LAI modeling. Compared with the LM, CART model produced better statistical performances with the same number and combination of explanatory variables. The high prediction power of CART suggests multivariate LAI assessments to be an alternative or supplement to more complex but univariate modeling approaches, e.g. as presented by Wang et al. (2016). Better agricultural management, relatively smaller field size and transplanted rice in KUL resulted in a higher homogeneity of plant. All these factors most likely reduced uncertainty in model predictions in comparison to the other sites (ELL, KAZ). They may limit the model transferability, not only between the sites, but also among different years as already indicated by Lee et al. (2017).

Conclusions

There are large spatial and temporal variations of biophysical parameters of rice at three sites. Multi-temporal Landsat-8 data enabled monitoring of vegetation growth through VIs. However, the different peaks of the rice VIs curves owed by crop growth stages in sites suggest to use separate scene dates of Landsat in order to model crop biophysical parameters at regional level. Further study is needed to investigate transferability of the CART model for other years and among the different sites (including practices).

Acknowledgements

This research is a part of the joint project "Assessing Land Value Changes and Developing a Discussion-Support-Tool for Improved Land Use Planning in the Irrigated Lowlands of Central Asia" (LaVaCCA), funded by the Volkswagen Foundation (Az. 88506). The authors thank all the personnel from the LaVaCCA project consortium involved in this study for their collaboration and data share.

References

Blenk S., 2005. Estimation of the leaf area index of cotton and rice from *in situ* observations... *Diploma Thesis*.
Breiman L., et al., 1984. Classification and regression trees. Boca Raton: Chapman & Hall/CRC.
Ehammer A., et al., 2010. Statistical derivation of FPAR and LAI for irrigated cotton and rice... Proceedings of *SPIE 782409*.
Fox J., Weisberg S., 2011. Multivariate Linear Models in R. An R Companion to Applied Regression, 2nd Edition.
Green I., Stephenson D., 1986. Criteria for comparison of single event models. *Hydro. Sci. J.* 31.
Lee B., et al., 2017. Evaluation of a phenology-dependent response method for estimating leaf area index of rice across climate gradients. *Remote Sens.* 9.
Liu, X., et al., 2017. Using an Active-Optical Sensor to Develop an Optimal NDVI Dynamic Model for High-Yield Rice Production (Yangtze, China). *Sensors* 17.
Pettorelli N., 2013. The normalized difference vegetation index. Oxford University Press, New York.
Ripley B., 2007. Tree: Classification and regression trees. R package version 1.0-26.
Wang J., et al., 2016. Dynamic mapping of rice growth parameters using HJ-1 CCD ... *Remote Sens.* 8.
Xue W., et al., 2017. Supplement understanding of the relative importance of biophysical factors in ... Agri. & Forest Meteorology 232.